

**Polar quasi-normal modes of neutron stars with equations of state satisfying the  $2 M_{\odot}$  constraint**J. L. Blázquez-Salcedo,<sup>1</sup> L. M. González-Romero,<sup>1</sup> and F. Navarro-Lérida<sup>2</sup><sup>1</sup>*Departamento de Física Teórica II, Facultad de Ciencias Físicas, Universidad Complutense de Madrid, 28040 Madrid, Spain*<sup>2</sup>*Departamento de Física Atómica, Molecular y Nuclear, Facultad de Ciencias Físicas, Universidad Complutense de Madrid, 28040 Madrid, Spain*

(Received 3 July 2013; published 6 February 2014)

In this paper, we analyze the quasinormal mode spectrum of realistic neutron stars by studying the polar modes. In particular, we calculate the fundamental mode (f mode), the fundamental pressure mode (p mode), and the fundamental curvature mode (wI mode) for 15 different equations of state satisfying the  $2 M_{\odot}$  constraint, most of them containing exotic matter. Since f and p modes couple to matter perturbations, the influence of the presence of hyperons and quarks in the core of the neutron stars is more significant than for the axial component. We present phenomenological relations, which are compatible with previous results, for the frequency and damping time with the compactness of the neutron star. We also consider new phenomenological relations between the frequency and damping time of the wI mode and the f mode. These new relations are independent of the equation of state and could be used to estimate the central pressure, mass, or radius and eventually constrain the equation-of-state of neutron stars. To obtain these results, we have developed a new method based on the exterior complex scaling technique with a variable angle.

DOI: [10.1103/PhysRevD.89.044006](https://doi.org/10.1103/PhysRevD.89.044006)

PACS numbers: 04.40.Dg, 04.30.-w, 95.30.Sf, 97.60.Jd

**I. INTRODUCTION**

Neutron stars can be used as probes to gain insight into the structure of matter at high densities ( $10^{15}$  g/cm<sup>3</sup> at their core). Knowledge on mass, radius, and any other global properties of the neutron star can give us important information on the state and composition of matter at those extreme physical conditions. However, although the mass can be determined with quite good precision, a direct measurement of the radius is currently very difficult using astrophysical observations.

Nevertheless, the detection of gravitational waves originated in the neutron stars could be used to obtain estimations, or at least constraints, on the value of the gravitational radius of the star. With knowledge on the mass and radius, we would be able to have a better understanding of the behavior of matter at high density and pressure. Therefore, the study of these gravitational waves is crucial in the understanding of the physics of matter at extreme densities.

Neutron stars present a layer structure, which can be essentially described by two very different regions: a core (where exotic matter could be found) enveloped by a *crust* (with a solid crystalline structure similar to a metal). The relativistic fluid that composes the neutron star can be described as a perfect fluid, for which the equation of state is needed. Because not much information is available beyond the nuclear densities, the equation of state is very model dependent, since different particle populations may appear at those energies [1,2]. Another interesting feature is that along the core of the star and especially in the core-crust interface first-order phase transitions could be found in realistic equations of state. These phase transitions result in small discontinuities in the energy density of the star matter [1,3].

Very interesting information can be obtained from the recent measurement of the mass of PSR J1614-2230, of  $1.97 M_{\odot}$ , which imposes constraints on equations of state for exotic matter that could be found in neutron stars [4]. Several equations of state that are able to produce neutron star configurations with  $2 M_{\odot}$  and exotic matter in their cores have been proposed [5–8]. If other global parameters could be measured, more important constraints could be imposed on the equation of state.

If an internal or external event perturbs a neutron star, it may oscillate nonradially, emitting gravitational waves to the space [9]. Large-scale interferometric gravitational wave detectors such as LIGO, GEO, TAMA, and VIRGO have reached the original design sensitivity, and the detection of the first gravitational waves could happen in the next few years [10]. These detections will provide useful information about the composition of the astrophysical objects that generate them, like neutron stars [9].

The gravitational waves emitted by a neutron star present dominant frequencies, which can be studied using the quasinormal mode formalism [11–13]. These eigenfrequencies are given by a complex number. The real part gives us the oscillation frequency of the mode, while the imaginary part gives us the inverse of the damping time. The quasinormal mode spectrum is quite dependent on the properties of the star, i.e., the equation of state.

Hence, the detection of gravitational radiation from neutron stars combined with a complete theoretical study of the possible spectra that can be obtained with different equations of state can be very useful in the determination of the matter behavior beyond nuclear matter [14–20].

The necessary formalism to study quasinormal modes was first developed for black holes by Regge and Wheeler [21]

and by Zerilli [22]. Quasinormal modes can be separated into polar and axial modes. The equation describing the quasinormal mode perturbation of the Schwarzschild metric is essentially a Schrödinger-like equation: the Regge–Wheeler equation for axial perturbations and the Zerilli equation for polar ones. For black holes, both types of modes are space-time modes. The formalism was first studied in the context of neutron stars by Thorne [23–27] and Lindblom [28,29] and then reformulated by Chandrasekhar and Ferrari [30–32], Ipser and Price [33], and Kojima [34]. In neutron stars, axial modes are purely space-time modes of oscillation (w modes), while polar modes can be coupled to fluid oscillations (fundamental f modes, pressure p modes, and also a branch of space-time w modes). In this paper, we will consider only polar modes of oscillation. The corresponding study of axial modes can be found in Ref. [35].

Although the perturbation equations for neutron stars can be simplified into a Regge–Wheeler equation or a Zerilli equation for the vacuum part of the problem, it is complicated to obtain the quasinormal mode spectrum of neutron stars. The equations must be solved numerically, and no analytical solution is known for physically acceptable configurations. The main difficulty is found on the diverging and oscillatory nature of the quasinormal modes. These functions are not handled well numerically.

Several methods have been developed to deal with these and other difficulties. For a complete review on the methods, see the review by Kokkotas and Schmidt [11].

The axial part of the spectrum has been extensively studied for simplified constant density models and polytropes [36–38]. Important results for the polar spectrum have been obtained using several methods, for example, the continued fraction method, which has been used to study realistic equations of state [14,16,20]. More recently, Samuelsson *et al.* [39] used a complex-radius approach for a constant density configuration to study axial quasinormal modes.

To use the results for future observations, Andersson and Kokkotas, first for polytropes [40] and later for some realistic equations of state [41], proposed some empirical relations between the modes and the mass and the radius of the neutron star that could be used together with observations to constrain the equation of state. In later works, Benhar, Ferrari, and Gualtieri [16,18,42] reexamined those relations for other realistic equations of state. Recently, the authors studied these relations for axial modes, using new equations of state satisfying the  $2 M_{\odot}$  condition [35].

In this work, we study similar relations for the polar modes that could be used to estimate global parameters of the star, constraining the equation of state of the core of the neutron star. We present a new approach to calculate quasinormal modes of realistic neutron stars. Essentially, it is the implementation to polar modes of the method used previously for axial modes in Ref. [35]. We make use of several well-known techniques, like the use of the phase for the exterior solution

and the use of a complexified coordinate to deal with the divergence of the outgoing wave. We also introduce some new techniques not used before in this context: freedom in the angle of the exterior complex path of integration, the use of the Colsys package to integrate all the system of equations at once with proper boundary and junction conditions, and the possibility of the implementation of phase transition discontinuities. These new techniques allow us to enhance accuracy, to obtain more modes in shorter times, and also to study several realistic equations of state, comparing results for different compositions.

In Sec. II, we present a brief review on the quasinormal mode formalism in order to fix notation. In Sec. III, we present the numerical method, which has been implemented in Fortran-based double-precision programs. In Sec. IV, we present the numerical results obtained from the application of the method and use them to study the realistic equations of state. We finish in Sec. V by presenting a summary of the main points of the paper.

## II. OVERVIEW OF THE FORMALISM

In this section, we will give a brief review of the formalism used to describe polar quasinormal modes and the method used to calculate them. Here and in the following section, we will use geometrized units ( $c = 1$ ,  $G = 1$ ).

We consider polar perturbations on the static spherical space-time describing the star:  $ds^2 = e^{2\nu} dt^2 - e^{2\lambda} dr^2 - r^2(d\theta^2 + \sin^2\theta d\varphi^2)$ . The matter is considered as a perfect fluid with a barotropic equation of state. As can be demonstrated, only polar modes do couple to the matter perturbations of the star [23–34], i.e., first-order perturbations of the energy density and pressure. Axial modes, which were studied in Ref. [35], are only coupled to the Lagrangian displacement of the matter. Therefore, the spectrum of polar modes is much more dependent on the matter content of the star than the axial modes.

Up to first order in perturbation theory, and once the gauge is fixed (Regge–Wheeler gauge [12]), the number of functions needed to describe the polar perturbations is 8, which are, following Lindblom notation [28,29],  $(H_{lm}^0, H_{lm}^1, H_{lm}^2, K_{lm}, W_{lm}, X_{lm}, \Pi_{lm}, E_{lm})$ . The Einstein equations, together with the conservation of energy and baryon number, can be reduced to four first-order differential equations for  $(H_{lm}^1, K_{lm}, W_{lm}, X_{lm})$  and four algebraic relations for  $(H_{lm}^0, H_{lm}^2, \Pi_{lm}, E_{lm})$ .

The angular dependence of the functions is known from the tensor expansion, and we will only consider in this work the  $l = 2$  case. We can extract the time dependence from the functions by making a Laplace transformation resulting in equations explicitly dependent on the eigenvalue  $\omega$ .

Inside of the star, we will need to solve the well-known zeroth-order system of equations for the hydrostatic equilibrium of a spherical star (Tolman–Oppenheimer–Volkoff equations):

$$\frac{dm}{dr} = 4\pi r^2 \rho, \quad (1)$$

$$\frac{dp}{dr} = -(\rho + p) \frac{m + 4\pi r^3 p}{(r - 2m)r}, \quad (2)$$

$$\frac{dv}{dr} = -\frac{1}{\rho + p} \frac{dp}{dr}. \quad (3)$$

Note that  $e^{-2\lambda(r)} = 1 - \frac{2m(r)}{r}$ . The total mass of the static configuration is  $M = \int_0^R dr 4\pi r^2 \rho$ , and the radius  $R$  of the star is defined where the pressure is zero  $p(R) = 0$ .

We need to specify the equation of state for the matter. Once we have a static solution, we can solve the system of four differential equations for the perturbations.

Outside the star (no matter), it can be seen that the system of equations can be rewritten, and it is reduced to a single second-order differential equation (Zerilli equation),

$$\frac{d^2 Z_{lm}}{dr_*^2} + [\omega^2 - V(r)] Z_{lm} = 0, \quad (4)$$

where  $r_*$  is the tortoise coordinate,

$$r_* = \int_0^r e^{\lambda - \nu} dr, \quad (5)$$

and the eigenfrequency of the polar mode is a complex number  $\omega = \omega_{\Re} + i\omega_{\Im}$ . As usual for quasinormal modes, we will consider  $\omega_{\Re} > 0$  and  $\omega_{\Im} > 0$ . The potential can be written as

$$V(r) = 2(r - 2M) \frac{n^2(n+1)r^3 + 3Mn^2r^2 + 9M^2nr + 9M^3}{r^4(nr + 3M)^2}, \quad (6)$$

where  $n = (l+2)(l-1)/2$  and  $l = 2$  in this work.

### III. NUMERICAL METHOD

Note that, in general, the perturbation functions are complex functions. So, numerically, we will have to integrate eight real first-order differential equations for the perturbation functions inside the star. These also translate into a set of two real second-order differential equations outside the star.

The perturbation has to satisfy a set of boundary conditions that can be obtained from the following two requirements [30]: (i) the perturbation must be regular at the center of the star, and (ii) the resulting quasinormal mode must be a pure outgoing wave.

In general, a quasinormal mode will be a composition of incoming and outgoing waves, i.e.,

$$\lim_{r_* \rightarrow \infty} Z^{\text{in}} \sim e^{i\omega r_*}, \quad \lim_{r_* \rightarrow \infty} Z^{\text{out}} \sim e^{-i\omega r_*}. \quad (7)$$

Note that, while the real part of  $\omega$  determines the oscillation frequency of the wave, the imaginary part of the eigenvalue determines the asymptotic behavior of the

quasinormal mode. Since  $\omega_{\Re} > 0$  and  $\omega_{\Im} > 0$ , outgoing quasinormal modes are divergent at radial infinity, while ingoing ones tend exponentially to zero as the radius grows. We should impose the solution to behave as a purely outgoing quasinormal mode at a very distant point. This has the inconvenience that any small contamination of the outgoing signal gives rise to an important incoming wave component.

We have adapted a method based on the exterior complex scaling method, which we will describe briefly in the following paragraphs. It is an adaptation to polar modes of the method previously employed for axial quasinormal modes [35].

Outside the star, and following Refs. [39,43], we study the phase function (logarithmic derivative of the Z function),

$$g = \frac{1}{Z} \frac{dZ}{dr}, \quad (8)$$

which does not oscillate toward asymptotic infinity. The differential equation we need to solve for the phase reads

$$\frac{dg}{dr} = -g^2 - \frac{2M}{r(r-2M)}g + \frac{r^2}{(r-2M)^2}(\omega^2 - V(r)). \quad (9)$$

Although the phase allows us to eliminate the oscillation, we cannot distinguish between the mixed incoming and outgoing waves and the purely outgoing ones. To do so, we can study an analytical extension of the phase function, rotating the radial coordinate into the complex plane,

$$r = R + ye^{-i\alpha}, \quad (10)$$

with  $y \in [0, \infty)$ . This technique of complexification of the integration variable is called exterior complex scaling [44–46].

Once a configuration is chosen, and a couple of values  $\omega_{\Re}$  and  $\omega_{\Im}$  are also chosen, then we take  $\alpha$  so that

$$\omega_{\Re} \sin \alpha + \omega_{\Im} \cos \alpha < 0. \quad (11)$$

If  $\alpha$  satisfies this relation, then it can be demonstrated [35] that for pure outgoing waves the boundary condition  $g(y = \infty) = -i\omega$  is satisfied. Instead, any solution containing any ingoing wave contribution will satisfy  $g(y = \infty) = i\omega$ . Hence, if the boundary condition  $g(y = \infty) = -i\omega$  is imposed on a particular solution outside the star, it must be a purely outgoing wave.

In our method, the angle  $\alpha$  is constrained by relation (11). Nevertheless, we can choose this angle freely satisfying  $\alpha > \arctan \frac{\omega_{\Im}}{\omega_{\Re}} \equiv \alpha_0$ . Typically, the accuracy can be increased and the integration time reduced if  $1 < \alpha/\alpha_0 < 1.5$ . Usually, for a particular family of modes, the optimum value of  $\alpha$  can be estimated at once for the maximum mass configuration.

The use of the phase and exterior complex scaling with variable angle allows us to compactify the radial coordinate

$$\bar{y} = \frac{y}{1+y}, \quad (12)$$

where  $\bar{y} \in [0, 1]$ . Hence, we can impose the outgoing quasinormal mode behavior as a boundary condition at infinity ( $g(\bar{y} = 1) = -i\omega$ ), without using any cutoffs for the radial coordinate.

The interior part is integrated satisfying the regularity condition at the origin. We integrate together the zeroth order and the Zerilli equation. In this way, we can automatically generate more points in the zeroth-order functions if we require a more accurate result in our quasinormal modes.

As we are interested in realistic equations of state, the implementation of the equation of state is a fundamental step of the procedure. We use two possibilities. The first one is a piecewise polytrope approximation, done by Read *et al.* [47] for 34 different equations of state, where each equation of state is approximated by a polytrope in different density-pressure intervals. For densities below the nuclear density, the Douching and Haensel [48] equation of state (SLy) is considered. The second kind of implementation for the equation of state, more general, is a piecewise monotonic cubic Hermite interpolation. We use this method to interpolate the density  $\rho$  as a function of the pressure satisfying local thermodynamic conditions [49]. The interpolation is made on several tabulated equations of state that we will present later.

We implement this method into different Fortran programs and routines, making use of the Colsys package [50] to solve numerically the differential equations. The advantage of this package is that it allows the use of quite flexible multiboundary conditions and an adaptive mesh that increases accuracy.

The matching of the interior and exterior solutions is performed on a surface  $S$ , defined by the points at which the pressure is null, or, more generally, constant. As we have mentioned previously, the polar oscillations modify the pressure and the density, so the surfaces of constant pressure of the perturbed star are given by the surfaces  $S$  of

$$p_{\text{total}} = p(r) + \Pi_{\text{lm}}(r, t)Y_{\text{lm}} = \text{const}, \quad (13)$$

where  $\Pi_{\text{lm}}$  is the perturbation of the pressure. In particular, the surface of the star is located where  $p_{\text{total}} = 0$ .

We calculate a vector normal to these surfaces,  $n^\mu$ , and from it the projector  $h_{\mu\nu} = g_{\mu\nu} + n_\mu n_\nu$  and the projected covariant derivative of the normal vector  $\chi_{\mu\nu} = h_\mu^\alpha h_\nu^\beta n_{\alpha;\beta}$ . Evaluating these tensors at a surface of constant pressure, from inside and from outside  $S$ , we obtain the first fundamental form and the second fundamental form inside and outside  $S$  [51]. We must make a series expansion of these conditions in order to obtain matching relations for each one of the metric functions. We also must expand in spherical harmonics and make a Laplace transformation, in order to obtain the junction of the radial component of the functions.

Let us consider a surface layer on top of  $S$  described by a surface stress-energy tensor of a perfect fluid of the form

$$T_S^{\mu\nu}(R) = \rho_c u_S^\mu(R) u_S^\nu(R), \quad (14)$$

where  $\rho_c = \varepsilon + \delta\varepsilon_{\text{lm}} Y_{\text{lm}}$  is the surface energy density of the fluid moving in  $S$  and  $u_S^\mu(R)$  is its velocity.

The second fundamental form conditions impose a jump in the pressure if  $\varepsilon \neq 0$ . Let the pressure in the inner part of the surface  $S$  be  $p_{\text{int}}$  and in the outer part be  $p_{\text{ext}}$  with  $p_{\text{ext}} < p_{\text{int}}$ .

At zeroth order, we obtain the following conditions:

$$\nu(R)|_{\text{int}} = \nu(R)|_{\text{ext}} \equiv \nu(R), \quad (15)$$

$$M_{\text{ext}} = M_{\text{int}} + 4\pi R^2 \sqrt{1 - \frac{2M_{\text{int}}}{R}} \varepsilon - 8\pi^2 R^3 \varepsilon^2, \quad (16)$$

$$\frac{M_{\text{ext}} + 4\pi R^3 p_{\text{ext}}}{R^2 \sqrt{1 - \frac{2M_{\text{ext}}}{R}}} - \frac{M_{\text{int}} + 4\pi R^3 p_{\text{int}}}{R^2 \sqrt{1 - \frac{2M_{\text{int}}}{R}}} = 4\pi\varepsilon. \quad (17)$$

The first-order perturbation functions must satisfy the following matching condition:

$$V_{\text{lm}}(R)|_{\text{ext}} = V_{\text{lm}}(R)|_{\text{int}} \equiv V_{\text{lm}}(R), \quad (18)$$

$$\Delta[K_{\text{lm}}(R)] - \frac{2}{R} \Delta\left[\frac{W_{\text{lm}}(R)}{e^\lambda}\right] + \frac{4}{e^{\nu(R)}} \Delta\left[\frac{X_{\text{lm}}(R)}{(1 + 8\pi R^2 p)e^{2\lambda} - 1}\right] = 0, \quad (19)$$

$$\Delta[W_{\text{lm}}(R)] = 2a^2 e^{-\nu(R)} \Delta\left[\frac{e^\lambda X_{\text{lm}}(R)}{(\rho + p)(8\pi R^2 p e^{2\lambda} + e^{2\lambda} - 1)}\right], \quad (20)$$

$$\Delta[e^{-\lambda} H_{\text{lm}}^1(R)] + 16\pi R^{-1} \varepsilon V_{\text{lm}}(R) = 0, \quad (21)$$

where  $\Delta[F(R)] = F(R)|_{\text{ext}} - F(R)|_{\text{int}}$ . Note that since we are matching with the exterior,  $X_{\text{lm}}(R)|_{\text{ext}} = 0$  [28,29]. Recall that in the previous expressions we allow for the possibility of surface energy density  $\varepsilon$  and jumps in pressure and density [35]. The standard matching conditions are reobtained when  $\varepsilon = 0$ .

The full solution is generated using two independent solutions of the perturbation equations for the same static configuration and value of  $\omega$ . Let us index each one of the independent solutions with a label  $i = \{A, B\}$ . If a linear combination of these two independent interior solutions matches the exterior phase, then we will have an outgoing quasinormal mode for the full solution.

We can always impose conditions (18), (20), and (21) on the two independent solutions. Then, it can be demonstrated that the junction can be written in terms of a determinant of a  $2 \times 2$  matrix,



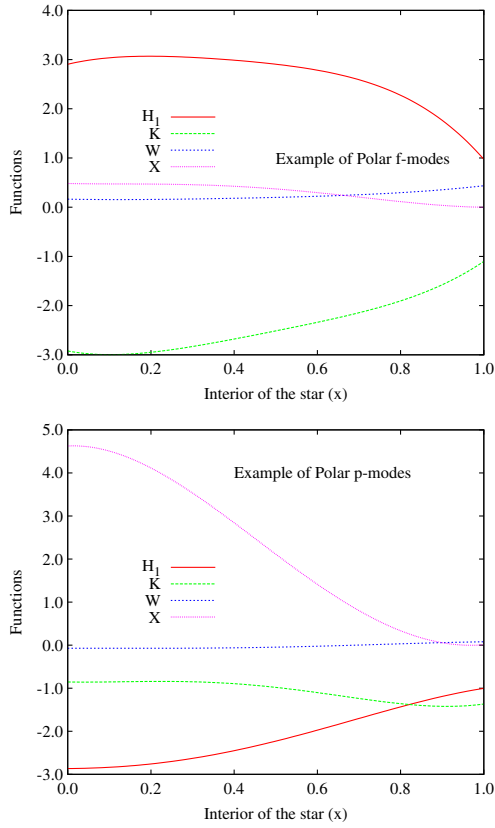


FIG. 1 (color online). Typical form of the functions integrated inside of the star for f modes and p modes ( $x = r/R$ ).

$$M_j^i = K_{\text{ext},(j)}^{(i)} - K_{\text{int},(j)}^{(i)} + \frac{2}{R^2}(e^{-\lambda_{\text{int}}} - e^{-\lambda_{\text{ext}}})W_{\text{int},(j)}^{(i)} + \frac{4[e^{2(\lambda_{\text{int}} - \lambda_{\text{ext}})} - 1]X_{\text{int},(j)}^{(i)}}{(8\pi R \rho_{\text{int}} e^{2\lambda_{\text{int}}} + e^{2\lambda_{\text{int}}} - 1)(\rho_{\text{int}} + p_{\text{int}})e^{\nu(R)}}, \quad (22)$$

where  $i = \{A, B\}$  and  $j = \{\mathfrak{N}, \mathfrak{S}\}$ . The determinant is zero only if the junction conditions are satisfied: a combination of the interior solutions can be matched to the exterior phase (an outgoing wave). The determinant of this matrix, once the static configuration is fixed, only depends on the values  $(\omega_{\mathfrak{N}}, \omega_{\mathfrak{S}})$ . Therefore, if for a fixed configuration a value of the eigenfrequency makes the determinant null, that couple of values  $(\omega_{\mathfrak{N}}, \omega_{\mathfrak{S}})$  corresponds to a quasinormal mode of the static configuration. Then, the behavior of the perturbation functions can be analyzed to deduce if the quasinormal mode is a wI mode, a p mode, or an f mode.

In Fig. 1, we show a particular solution for the interior of a neutron star of  $1.4 M_{\odot}$ , equation of state GNH3. They correspond to the f mode and the fundamental p mode.

#### IV. RESULTS

In this section, we present our results for the polar quasinormal modes of neutron stars with realistic equations of state. We consider a wide range of equations of state in order to study the influence of exotic matter on the polar

quasinormal modes. For a similar study performed on the axial component of the spectra, see Ref. [35].

We have tested our method for the constant density model, reproducing the results from Ref. [52]. We have also tested our results for the APR2 equation of state. Our calculations for the real part are in perfect agreement with the results presented in Ref. [16]. The imaginary part is reproduced with a 1% difference for the maximum mass configurations, up to 10%–20% for the softer configurations. This is also expected due to the different methods used in the parametrization of the equation of state, determination of the radius, and quasinormal modes calculation.

As we will see, another test of our method is in the parameters of the empirical relations of the quasinormal modes we calculate. For the equations of state we consider, the parameters of the empirical relations are compatible with the ones obtained by Benhar *et al.* [14,16] for different equations of state.

We start presenting the equations of state used in the study. Using the parametrization presented by Read *et al.* [47], we have considered SLy, GNH3, H4, ALF2, ALF4.

After the recent measurement of  $1.97 M_{\odot}$  for the pulsar PSR J164-2230, several new equations of state have been proposed. These equations of state take into account the presence of exotic matter in the core of the neutron star, and they have a maximum mass stable configuration over  $1.97 M_{\odot}$ . We have considered the following ones: two equations of state presented by Weissenborn *et al.* with hyperons in Ref. [7], which we call WCS1 and WCS2; three equations of state presented by Weissenborn *et al.* with quark matter in Ref. [8], which we call WSPHS1, WSPHS2, and WSPHS3; four equations of state presented by Bonanno and Sedrakian in Ref. [6], which we call BS1, BS2, BS3, and BS4; and one equation of state presented by Bednarek *et al.* in Ref. [5], which we call BHZBM.

In Fig. 2, we plot all 15 equations of state we have studied in order to give an idea of the range considered.

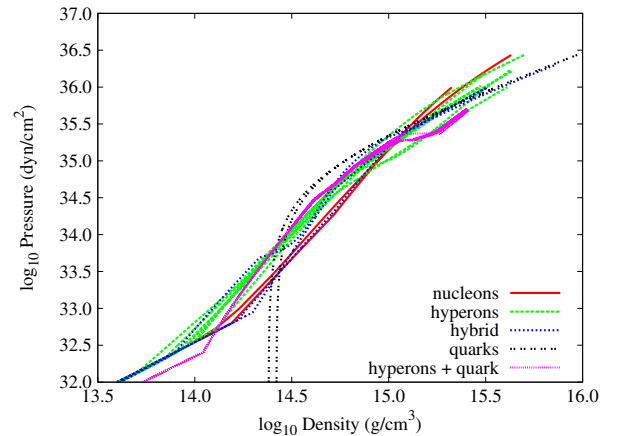


FIG. 2 (color online). Pressure vs density in logarithmic scale for the 15 equations of state considered, in the high density region.

We follow the notation previously used in Ref. [35]. We discuss their characteristics in the following paragraph.

For plain  $npe\mu$  nuclear matter, we use:

- (i) SLy [48] with  $npe\mu$  using a potential method to obtain the equation of state.

For mixed hyperon-nuclear matter, we use:

- (i) GNH3 [53], a relativistic mean-field theory equation of state containing hyperons;
- (ii) H4 [54], a variant of the GNH3 equation of state;
- (iii) WCS1 and WCS2 [7], two equations of state with hyperon matter, using “model  $\sigma\omega\rho\phi$ ,” and considering ideal mixing, the SU(6) quark model, and the symmetric-antisymmetric couplings ratios  $\alpha_v = 1$  and  $\alpha_v = 0.2$ , respectively.

- (iv) BHZBM [5], a nonlinear relativistic mean-field model involving a baryon octet coupled to meson fields.

For hybrid stars, we use:

- (i) ALF2 and ALF4 [55], two hybrid equations of state with mixed nuclear matter and color-flavor-locked quark matter;
- (ii) WSPHS3 [8], a hybrid star calculated using a bag model, mixed with NL3 RMF hadronic equations of state, and the parameters employed are  $B_{\text{eff}}^{1/4} = 140$  MeV,  $a_4 = 0.5$ , and a Gibbs phase transition.

For Hybrid stars with hyperons and quark color superconductivity, we use:

- (i) BS1, BS2, BS3, and BS4, [6], four equations of state calculated using a combination of a phenomenological relativistic hypernuclear density functional and an effective Nambu-Jona-Lasinio model of quantum chromodynamics, and the parameters considered are vector coupling  $G_V/G_S = 0.6$  and quark-hadron transition density  $\rho_{tr}/\rho_0$  equal to 2, 3, 3.5, and 4, respectively, where  $\rho_0$  is the density of nuclear saturation.

For quark stars, we use:

- (i) WSPHS1 and WSPHS2 [8], and the first equation of state is for unpaired quark matter, and we have considered the parameters  $B_{\text{eff}}^{1/4} = 123.7$  MeV,  $a_4 = 0.53$ ; the second equation of state considers quark matter in the color-flavor-locked phase (paired), and the parameters considered are  $B_{\text{eff}}^{1/4} = 130.5$  MeV,  $a_4 = 0.66$ , and  $\Delta = 50$  MeV.

In Fig. 3, we plot the frequencies of all the f modes, p modes, and wI0 modes we have calculated using our method, for the 15 equations of state considered, in order to present the range in which each mode is found. In the next subsections, we will explain the features of each class of modes depending on the equation of state composition: hyperon matter or quark matter.

## A. Hyperon matter

### 1. Fundamental wI mode

At the maximum mass configuration of each equation of state (around  $2 M_\odot$ ), all the equations of state yield

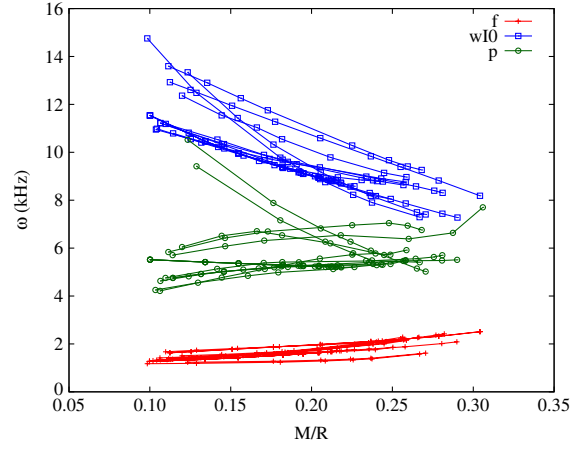


FIG. 3 (color online). Frequency vs compactness for all the modes calculated in this work.

frequencies near 8.5 kHz. This is found for stars containing hyperon matter or only nuclear matter. The only exception is the interesting case of the WCS2 (maximum mass of  $2.4 M_\odot$ ) with the smallest frequency (7.5 kHz). In general, for configurations with one solar mass, the frequency of stars containing hyperon matter is much smaller (11 kHz) than the frequencies for plain nuclear matter stars (14 kHz).

To use future observations of gravitational waves to estimate the mass and the gravitational radius of the neutron star, as well as to discriminate between different families of equations of state, we obtain empirical relations between the frequency and damping time of quasinormal modes and the compactness of the star, following Refs. [14–16,40,41]. In Fig. 4, we present the frequency of the fundamental mode scaled to the radius of each configuration. The range of the plot is between  $1 M_\odot$  and the maximum mass configuration, so we consider only stable stars. It is interesting to note that even for the softest

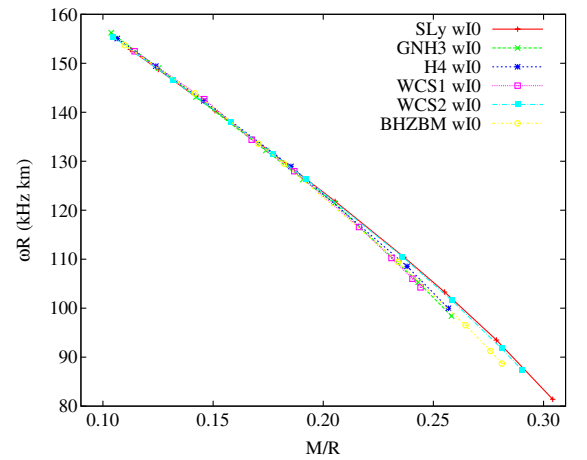


FIG. 4 (color online). Scaled frequency of the fundamental wI mode vs  $M/R$  for hyperon matter equations of state. The phenomenological relation is quite independent of the matter composition, as expected from spatial modes.

TABLE I. Fits for the wI0 modes for hyperon equations of state. Parameters  $A$  and  $B$  ( $\text{kHz} \times \text{km}$ ) correspond to the linear empirical relation for the frequency (23). Parameters  $a$ ,  $b$ , and  $d$  ( $\text{kHz} \times (\mu\text{s})^{-1}$ ) correspond to the quadratic empirical relation for the damping time (24). Pure nucleonic matter equation of state SLy is included for comparison.

wI0	SLy	GNH3	H4	WCS1	WCS2	BHZBM
$A$	$-365.3 \pm 8.2$	$-371.0 \pm 8.6$	$-364.4 \pm 1.6$	$-374.4 \pm 8.2$	$-365.2 \pm 7.2$	$-384.2 \pm 8.2$
$B$	$195.3 \pm 1.8$	$195.9 \pm 1.6$	$194.9 \pm 1.6$	$196.7 \pm 1.6$	$195.3 \pm 1.5$	$198.0 \pm 1.8$
$\chi^2$	2.523	1.547	1.479	1.06	1.84	2.03
$a$	$-155 \pm 31$	$-339 \pm 31$	$-330 \pm 35$	$-401 \pm 16$	$-217 \pm 30$	$-253 \pm 41$
$b$	$-11 \pm 13$	$49 \pm 11$	$48 \pm 13$	$70 \pm 6$	$13 \pm 12$	$21 \pm 17$
$d$	$19.7 \pm 1.3$	$15.1 \pm 1.0$	$15.1 \pm 1.1$	$13.34 \pm 0.51$	$17.6 \pm 1.2$	$17.2 \pm 1.6$
$\chi^2$	0.10	0.041	0.0308	0.005	0.0827	0.0968

equations of state with hyperon matter the scaling relation is very well satisfied. Since the wI modes do not couple to matter oscillations, it is not a surprise that these scaled relations are universal.

A linear fit can be made for each equation of state. We fit to the phenomenological relation

$$\omega(\text{kHz}) = \frac{1}{R(\text{km})} \left( A \frac{M}{R} + B \right), \quad (23)$$

where  $A$  and  $B$  are given in  $\text{kHz} \times \text{km}$ . Note  $\frac{M}{R}$  is dimensionless. We are choosing the units so that we can compare our fits with the results from Ref. [16]. In this section, we will express the fit parameters of the phenomenological relations following the units from Ref. [16], which are appropriate in an astrophysical context.

In Table I, we present the fit parameters  $A$ ,  $B$  for each one of the equations of state studied. For all the equations of state, very similar results are obtained. The empirical parameters are compatible with the empirical relation obtained by Benhar *et al.* [16] for six different equations of state.

A similar study can be done to the damping time of the wI0 modes. In Fig. 5 we present the damping time of the fundamental mode scaled to the mass of each configuration. In this case, the results can be fitted to a empirical quadratic relation on  $M/R$  as

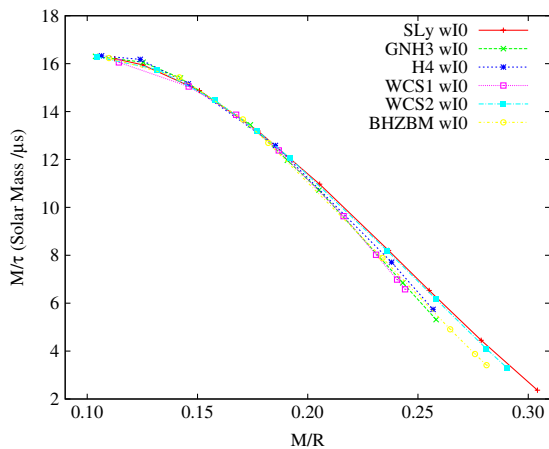


FIG. 5 (color online). Scaled damping time of the fundamental wI mode vs  $M/R$  for hyperon matter equations of state.

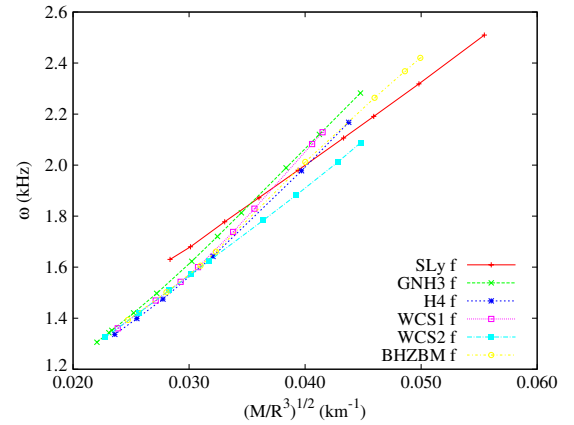


FIG. 6 (color online). Scaled frequency of the fundamental f mode vs  $\sqrt{M/R^3}$  for hyperon matter. Although the frequency is linear with the square root of the mean density, each equation of state has its own particular phenomenological parameters, and so the empirical relation is less useful in asteroseismology.

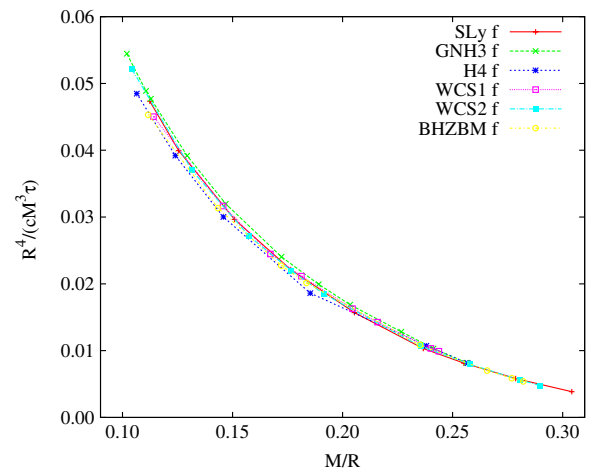


FIG. 7 (color online). Scaled damping time of the fundamental f mode vs  $M/R$  for hyperon matter. In this case, the scaled damping time is quite independent of the equation of state.

TABLE II. Fits for the f modes for hyperon equations of state. Parameters  $U$  (in kHz) and  $V$  (in kHz  $\times$  km) correspond to the linear empirical relation for the frequency (25). Parameters  $u$  and  $v$  (dimensionless) correspond to the linear empirical relation for the damping time (26). Pure nucleonic matter equation of state SLy is included for comparison.

f	SLy	GNH3	H4	WCS1	WCS2	BHZBM
$U$	$0.7041 \pm 0.0063$	$0.338 \pm 0.018$	$0.337 \pm 0.055$	$0.257 \pm 0.055$	$0.5330 \pm 0.0083$	$0.328 \pm 0.026$
$V$	$32.44 \pm 0.15$	$43.07 \pm 0.55$	$41.5 \pm 1.1$	$44.5 \pm 1.6$	$34.52 \pm 0.24$	$41.93 \pm 0.68$
$\chi^2$	$1.58 \times 10^{-5}$	$1.82 \times 10^{-4}$	$3.75 \times 10^{-4}$	$7.41 \times 10^{-4}$	$2.77 \times 10^{-5}$	$3.14 \times 10^{-4}$
$u$	$0.065 \pm 0.005$	$0.079 \pm 0.004$	$0.071 \pm 0.006$	$0.070 \pm 0.004$	$0.067 \pm 0.006$	$0.063 \pm 0.005$
$v$	$-0.221 \pm 0.023$	$-0.295 \pm 0.021$	$-0.255 \pm 0.030$	$-0.251 \pm 0.022$	$-0.231 \pm 0.021$	$-0.213 \pm 0.021$
$\chi^2$	$1.98 \times 10^{-5}$	$1.32 \times 10^{-5}$	$1.72 \times 10^{-5}$	$7.18 \times 10^{-6}$	$2.42 \times 10^{-5}$	$1.33 \times 10^{-5}$

$$\frac{1}{\tau(\mu s)} = \frac{1}{M(M_\odot)} \left[ a \left( \frac{M}{R} \right)^2 + b \frac{M}{R} + d \right], \quad (24)$$

where  $a$ ,  $b$ , and  $d$  are given in  $M_\odot \times (\mu s)^{-1}$ . Here, again, we are choosing the units like in Ref. [16]. In Table I, we present the fit parameters  $a$ ,  $b$ , and  $d$ . Note that they are quite similar for all the equations of state and also in accordance with the results obtained in Ref. [16].

For a similar study of the axial wI modes using these equations of state, see Ref. [35].

### 2. f mode

Now, we will present the results for the f modes of these configurations. For these modes, the frequency of

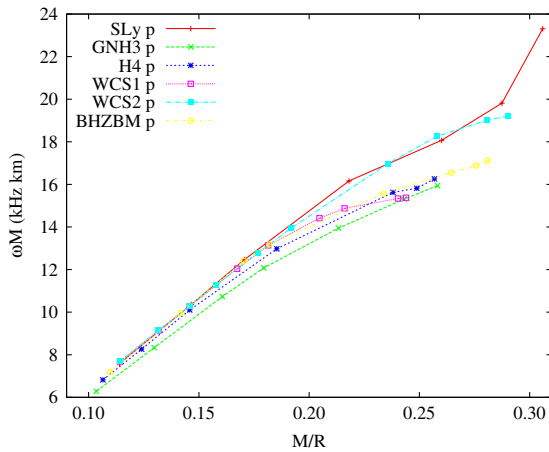


FIG. 8 (color online). Scaled frequency of the fundamental p mode vs  $M/R$ . At high compactness the scaled frequency is more sensible to the presence of hyperon matter, with the exception of WCS2.

TABLE III. Fits for the p modes for hyperon equations of state. Parameters  $K$  and  $K_0$  (kHz  $\times$  km) correspond to the linear empirical relation for the frequency (27). Pure nucleonic matter equation of state SLy is included for comparison.

p	SLy	GNH3	H4	WCS1	WCS2	BHZBM
$K$	$74.9 \pm 4.5$	$62.2 \pm 3.3$	$61.8 \pm 3.3$	$59.8 \pm 4.8$	$66.8 \pm 2.7$	$54.4 \pm 4.5$
$K_0$	$-0.68 \pm 1.0$	$0.368 \pm 0.634$	$0.74 \pm 0.64$	$1.54 \pm 0.90$	$0.616 \pm 0.553$	$2.33 \pm 0.96$
$\chi^2$	0.65	0.218	0.249	0.401	0.260	0.590

the SLy stars is always above the hyperon stars considered. The SLy configurations range from 1.6 kHz for  $1 M_\odot$  to 2.5 kHz for the maximum mass configuration. Hyperon stars range from 1.3 kHz for  $1 M_\odot$  to 2.2 kHz, with again the exception of WCS2, which reaches only 2.1 kHz.

In this case, one can also study some empirical relations. It is interesting to study the dependence of the frequency with the square root of the mean density. The empirical relations considered for the f modes are the following. For the frequency,

$$\omega(\text{kHz}) = U + V \sqrt{\frac{M}{R^3}}, \quad (25)$$

where  $U$  is given in kHz and  $V$  in kHz  $\times$  km. Note that the mean density  $\frac{M}{R^3}$  is given in  $(\text{km})^{-2}$ . For the damping time,

$$\tau(\text{s}) = \frac{R^4}{cM^3} \left[ u + v \frac{M}{R} \right]^{-1}, \quad (26)$$

where  $u$  and  $v$  are dimensionless parameters,  $M$  and  $R$  are given in km, and  $c = 2.99792458 \times 10^5$  km/s is the speed of light. For these formulas, we have chosen dimensions like in Benhar *et al.* [16]. In Figs. 6 and 7, we plot these relations. In Fig. 6, it can be seen that Eq. (25) is quite different depending on the equation of state. Again, WCS2 presents a very different behavior close to the maximum mass configurations. For the damping time, relation (26) is very well satisfied for every equation of state along all the range.

In Table II, we present the fit parameters  $U$  and  $V$  for the frequency and  $u$  and  $v$  for the damping time. These empirical parameters are compatible with those obtained by Benhar *et al.* [16] for six different equations of state.



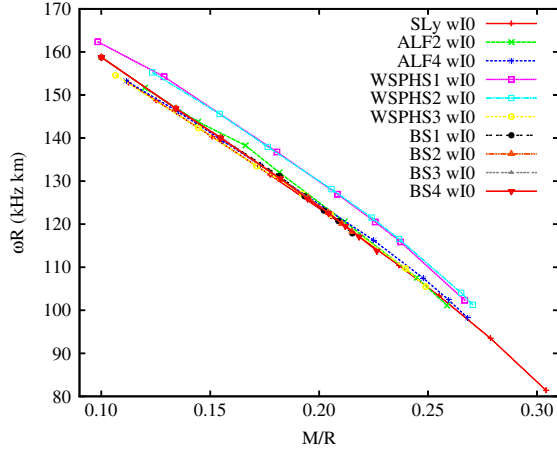


FIG. 9 (color online). Scaled frequency of the fundamental wI mode vs  $M/R$  for equations of state containing quarks. Note that the pure quark configurations of equations of state WSPHS1–WSPHS2 present a different set of phenomenological parameters.

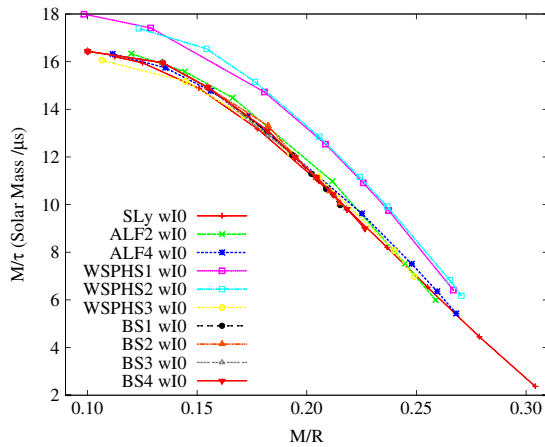


FIG. 10 (color online). Scaled damping time of the fundamental wI mode vs  $M/R$  for equations of state containing quarks. Hybrid and quark stars have different parameters in the empirical relations.

### 3. Fundamental $p$ mode

The frequency of the fundamental  $p$  mode is the most sensitive to the equations of state of the configuration. For the SLy equation of state, the frequency ranges from 5.7 kHz for  $1 M_{\odot}$  to 7.8 kHz for the maximum mass configuration. In the presence of hyperon matter, the range of frequencies is much shorter, varying from 4.6 kHz for  $1 M_{\odot}$  to 5.5 kHz for the maximum mass configuration.

In principle, selecting the units like in Ref. [16], an interesting empirical relation is

$$\omega(\text{kHz}) = \frac{1}{M(\text{km})} \left( K \frac{M}{R} + K_0 \right), \quad (27)$$

where  $K$  and  $K_0$  are given in  $\text{kHz} \times \text{km}$ . In Fig. 8, we present the frequency scaled to the mass vs the compactness. There is an important resemblance between the SLy equation of state and the WCS2, which presents a similar behavior for high compact stars. The relation is quite different from the rest of hyperon matter equations of state. This effect could be used to constrain the value of  $\alpha_v$  for compact enough stars.

In Table III, we present the fit parameters  $K$  and  $K_0$  for the frequency. The results are compatible with Ref. [16].

## B. Quark matter

### 1. Fundamental wI mode

The frequencies for the hybrid equation of state ALF4 give almost the same results as the SLy equation of state. The four BS1–BS4 equations of state are essentially similar, with quite a low frequency: 8.8 kHz for the maximum mass configuration ( $2 M_{\odot}$ ). Nevertheless, the WSPHS3 is the equation of state with the lowest frequency: 8 kHz for the maximum mass configuration ( $2.2 M_{\odot}$ ). For pure quark stars WSPHS1–WSPHS2, even lower frequencies (7.2 kHz) are obtained at the maximum mass configuration ( $2.5 M_{\odot}$ ).

We study the empirical relations (23) and (24) for these equations of state. We present them in Figs. 9 and 10 for frequency and damping time, respectively. It can be seen

TABLE IV. Fits for the wI0 modes for quark and hybrid equations of state. Parameters  $A$  and  $B$  ( $\text{kHz} \times \text{km}$ ) correspond to the linear empirical relation for the frequency (23). Parameters  $a$ ,  $b$ , and  $d$  ( $\text{kHz} \times (\mu\text{s})^{-1}$ ) correspond to the quadratic empirical relation for the damping time (24).

wI0	ALF2	ALF4	WSPHS1	WSPHS2	WSPHS3	BS1	BS2	BS3	BS4
$A$	$-365.3 \pm 11.9$	$-368.9 \pm 6.7$	$-351.9 \pm 12.3$	$-365.5 \pm 10.3$	$-342.1 \pm 6.7$	$-351.4 \pm 4.7$	$-350.0 \pm 0.30$	$349.6 \pm 2.7$	$353.2 \pm 3.2$
$B$	$197.1 \pm 2.3$	$193.3 \pm 1.4$	$199.0 \pm 2.5$	$202.0 \pm 2.2$	$191.8 \pm 1.3$	$194.2 \pm 0.8$	$193.9 \pm 0.5$	$194.4 \pm 0.6$	
$\chi^2$	2.227	1.164	3.326	2.039	0.687	0.251	0.11	0.086	0.149
$a$	$-347 \pm 18$	$-281 \pm 19$	$-333.9 \pm 8.7$	$-332 \pm 24$	$-339 \pm 21$	$-339 \pm 21$	$-473 \pm 21$	$-492 \pm 29$	$-432 \pm 34$
$b$	$56.1 \pm 6.9$	$35.9 \pm 7.4$	$52.6 \pm 3.2$	$53.1 \pm 9.6$	$56.3 \pm 7.6$	$92.3 \pm 6.6$	$99.0 \pm 9.2$	$80 \pm 11$	$79.9 \pm 8.0$
$d$	$14.66 \pm 0.63$	$15.93 \pm 0.67$	$16.10 \pm 0.27$	$16.03 \pm 0.92$	$13.97 \pm 0.65$	$11.98 \pm 0.51$	$11.46 \pm 0.71$	$12.79 \pm 0.85$	$12.82 \pm 0.63$
$\chi^2$	0.0079	0.013	0.0037	0.0204	0.0133	0.0049	0.0096	0.0148	0.0102

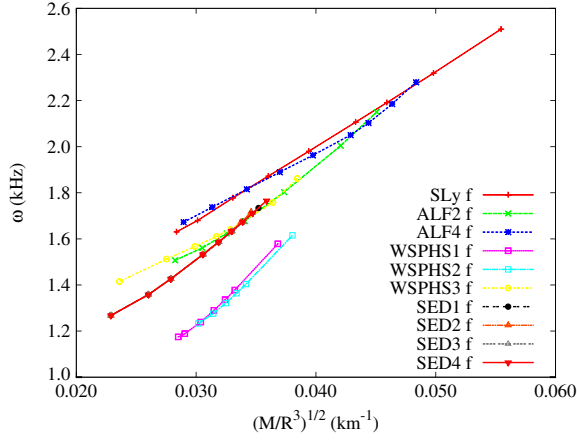


FIG. 11 (color online). Scaled frequency of the fundamental  $f$  mode vs  $\sqrt{M/R^3}$  for equations of state containing quarks. In this case, the empirical relation is dependent of the equation of state considered, and so it is less useful in asteroseismology.

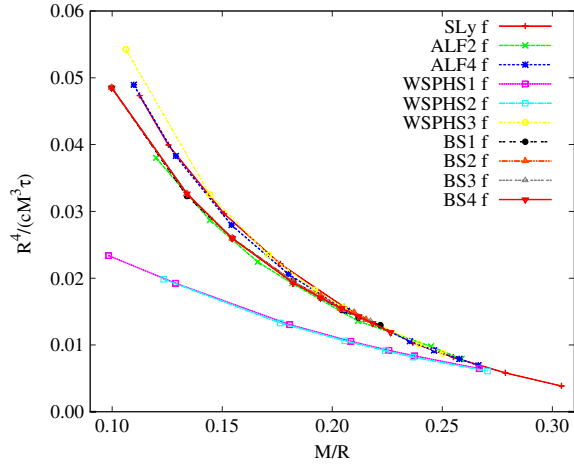


FIG. 12 (color online). Scaled damping time of the fundamental  $f$  mode vs  $M/R$  for hybrid and quark stars. The empirical relation is almost insensitive of the equation of state, except for the pure quark stars.

that the empirical relation is again very well satisfied for all the hybrid equations of state. For the pure quark stars, a similar relation with different parameters is found. The fits can be found in Table IV (compatible with Ref. [16]).

TABLE V. Fits for the  $f$  modes for quark and hybrid equations of state. Parameters  $U$  (in kHz) and  $V$  (in kHz  $\times$  km) correspond to the linear empirical relation for the frequency (25). Parameters  $u$  and  $v$  (dimensionless) correspond to the linear empirical relation for the damping time (26).

$f$	ALF2	ALF4	WSPHS1	WSPHS2	WSPHS3	BS1	BS2	BS3	BS4
$U$	$0.38 \pm 0.06$	$0.79 \pm 0.04$	$-0.24 \pm 0.07$	$-0.28 \pm 0.07$	$0.71 \pm 0.06$	$0.37 \pm 0.04$	$0.36 \pm 0.04$	$0.38 \pm 0.04$	$0.36 \pm 0.03$
$V$	$38.7 \pm 1.6$	$30.0 \pm 1.1$	$48.9 \pm 2.1$	$49.4 \pm 2.1$	$29.2 \pm 1.9$	$98.3 \pm 1.2$	$38.6 \pm 1.3$	$37.9 \pm 1.1$	$38.8 \pm 1.1$
$\chi^2$	$6.03 \times 10^{-4}$	$4.66 \times 10^{-4}$	$2.15 \times 10^{-4}$	$1.67 \times 10^{-4}$	$5.58 \times 10^{-4}$	$1.69 \times 10^{-4}$	$2.04 \times 10^{-4}$	$1.58 \times 10^{-4}$	$1.77 \times 10^{-5}$
$10u$	$0.59 \pm 0.04$	$0.70 \pm 0.05$	$0.32 \pm 0.01$	$0.31 \pm 0.02$	$0.79 \pm 0.08$	$0.72 \pm 0.04$	$0.73 \pm 0.04$	$0.73 \pm 0.04$	$0.71 \pm 0.04$
$v$	$0.21 \pm 0.02$	$0.25 \pm 0.02$	$0.10 \pm 0.01$	$0.09 \pm 0.01$	$0.30 \pm 0.04$	$0.28 \pm 0.03$	$0.29 \pm 0.02$	$0.28 \pm 0.02$	$0.27 \pm 0.02$
$\chi^2$	$6.91 \times 10^{-6}$	$1.45 \times 10^{-5}$	$7.74 \times 10^{-7}$	$6.69 \times 10^{-7}$	$2.48 \times 10^{-5}$	$7.55 \times 10^{-6}$	$6.58 \times 10^{-6}$	$6.84 \times 10^{-6}$	$7.03 \times 10^{-6}$

Note that, although the empirical relation is also satisfied for pure quark stars, it is slightly different. This is due to the different layer structure of these pure quark stars. These stars are essentially naked quark cores, where the pressure quickly drops to zero in the outer layers, although the density is almost constant.

The study of the axial  $wI$  modes using these equations of state can be found in Ref. [35].

## 2. $f$ mode

The lowest frequency is around 1.2 kHz for  $1 M_\odot$  stars composed only of quark matter (WSPHS1–WSPHS2). The higher frequencies are reached at 2.2 kHz for hybrid stars beyond  $2 M_\odot$ . For ALF2–ALF4, frequencies approach those of pure nuclear matter. The configurations with equations of state WSPHS3 and BS1–BS4 always have lower frequencies than the rest of hybrid stars but are larger than the pure quark stars. Concerning the damping time, there is essentially no difference among the equations of state (0.3 s for maximum mass configurations), except for WSPHS1–WSPHS2, which have slightly larger damping times for the most compact ones (0.4 s for maximum mass configurations).

We study the dependence of the frequency with the square root of the mean density as we did before for hyperon matter. The empirical relations to consider are again Eqs. (25) and (26). In Figs. 11 and 12, we plot these relations. In Fig. 11, it can be seen that Eq. (25) is quite different, depending on the equation of state. ALF4 is almost identical to SLy, while the other hybrid equations are in between these ones and the pure quark equations of state. Regarding the damping time (Fig. 12), relation (26) is very well satisfied for every hybrid equation of state considered along all the range. These relations are compatible with Ref. [16]. In Table V, we present the fits to Eqs. (25) and (26) of these results.

## 3. Fundamental $p$ mode

At high compactness, ALF4 has higher frequencies (near 7 kHz) than the rest of hybrid equations of state (for example, BS1–BS4 and WSPHS1–WSPHS2 have similar frequencies around 5.2 kHz). The highest frequencies are reached for pure quark stars at  $1 M_\odot$ , with 10 kHz.

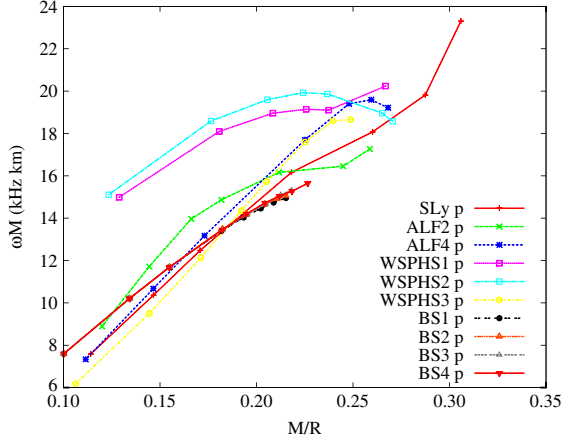


FIG. 13 (color online). Scaled frequency of the fundamental p mode vs  $M/R$ . Once again, a general tendency is seen, but the particular phenomenological relation of each equation of state is different from the rest. As expected, the p mode is very sensitive to the equation of state.

In Fig. 13 we present the empirical relations (27). It can be seen that all hybrid equations lie on the same range, although the linear relation is not very well satisfied for higher compactness. In the case of pure quark stars, the situation is much worse. In Table VI, we present the fits to Eq. (27) for each equation of state. These results are also compatible with Ref. [16].

### C. Universal phenomenological relations

To use wave detections coming from neutron stars to estimate global properties like radius or mass, we would like to have empirical relations as much independent from the matter content of the configuration as possible. The empirical relations for the wI modes are quite universal and hence are useful for asteroseismology. On the other hand, the scaled relations for the f mode are still equation of state dependent, especially for the frequency. Here we propose some new phenomenological relations that we think could be useful for asteroseismology.

First, we present a new empirical relation for the wI fundamental mode. A similar empirical relation for the axial wI modes was first studied in Ref. [35].

As seen in Fig. 14, if the real and the imaginary parts are scaled as

$$\bar{\omega}_R = \frac{1}{\sqrt{p_c}} \omega_R, \quad \bar{\omega}_I = \frac{1}{\sqrt{p_c}} \omega_I, \quad (28)$$

that is, normalized in units of the central pressure, then we obtain the following relation between real and imaginary parts of the eigenvalue for all the equations of state (except for WCSHS1–WCSHS2),

$$\bar{\omega}_I = (6.146 \pm 0.039)10^{-3} \bar{\omega}_R^2 + (-5.57 \pm 0.18)10^{-7} \bar{\omega}_R^4, \quad (29)$$

with  $\chi^2 = 0.0214$ . The relation is very well satisfied independently of the equation of state, in particular, for high-density stars. This could be used to estimate the central pressure of the star.

Note that although the empirical relation between  $\bar{\omega}_R$  and  $\bar{\omega}_I$  is quite independent of the equation of state, the parametrization of the curve in terms of the central pressure is equation of state dependent. If the frequency  $\omega$  and the damping time  $\tau$  are known (detected), we can parametrize a line defining  $\bar{\omega}_R$  and  $\bar{\omega}_I$ , with parameter  $p_c$ , using the observed frequency and damping time. The observed values will give us the slope of the line. The crossing point of this line with the empirical relation presented in Fig. 14 gives us an estimation of the central pressure  $p_c$  independent of the equation of state. Now, we can check which equation of state is compatible with this  $p_c$ , i.e., which one has the measured wI0 mode near the crossing point for the estimated central pressure. Hence, this method could be used to constrain the equation of state. Note that if mass and radius are already measured, we would have another filter to impose on the equation of state.

As a practical test of this method, we have included in Fig. 14 the line that a measurement of a fundamental wI0 mode of  $\omega = 11$  kHz and  $\tau = 118.4 \mu\text{s}$  will trace. The crossing point between this line and the empirical relation for the wI0 modes (29) determines the central pressure, yielding  $p_c = 1.312 \times 10^{35}$  dyn/cm<sup>2</sup>.

Concerning the f mode, an analogous relation can be obtained if we divide the real part and the imaginary part by the radius and mass, respectively. The empirical relation obtained is equation of state independent (excluding again WSPHS1–WSPHS2). It is

TABLE VI. Fits for the p modes for quark and hybrid equations of state. Parameters  $K$  and  $K_0$  (kHz  $\times$  km) correspond to the linear empirical relation for the frequency (27).

p	ALF2	ALF4	WSPHS1	WSPHS2	WSPHS3	BS1	BS2	BS3	BS4
$K$	$54.5 \pm 8.9$	$79.9 \pm 5.0$	$36.1 \pm 5.3$	$22.8 \pm 10.1$	$92.1 \pm 3.0$	$64.1 \pm 2.4$	$65.0 \pm 2.2$	$65.1 \pm 2.0$	$63.7 \pm 2.2$
$K_0$	$3.86 \pm 1.73$	$-1.0 \pm 1.1$	$10.9 \pm 1.1$	$13.8 \pm 2.2$	$-3.56 \pm 0.60$	$1.5 \pm 0.4$	$1.38 \pm 0.40$	$1.36 \pm 0.35$	$1.58 \pm 0.41$
$\chi^2$	1.24	0.556	0.322	1.66	0.153	0.067	0.059	0.047	0.072

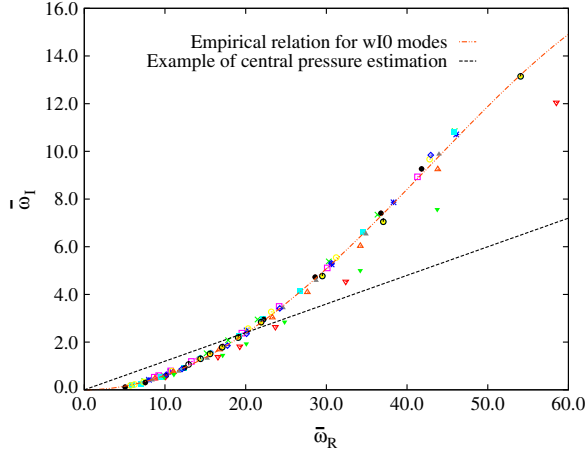


FIG. 14 (color online). All fundamental wI modes normalized to the square root of the central pressure [Eq. (28)]. This scaling makes all the wI0 modes lie on the same curve and could be used to estimate the central pressure as explained in the text.

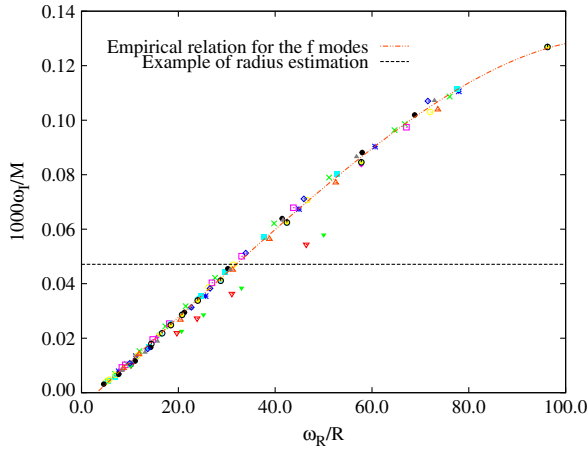


FIG. 15 (color online). All fundamental f modes. The real part of the eigenvalue is divided by the radius and the imaginary part by the mass. This universal relation can be very useful to estimate the radius or mass of a neutron star. Note that all the equations of state, with the exception of the pure quark stars, are found to satisfy the empirical relation (30).

$$\begin{aligned}
 (\omega_I/M) = & (-5.16 \pm 0.24)10^{-3} + (164.63 \pm 0.83)10^{-5} \\
 & \times (\omega_R/R) + (-3.14 \pm 0.12)10^{-10}(\omega_R/R)^4,
 \end{aligned}
 \tag{30}$$

with  $\chi^2 = 1.42 \times 10^{-6}$ . It is an almost linear relation, although the  $(\omega_R/R)^4$  plays an important role at low compactness configurations. This relation is very well satisfied for every configuration independently of the equation of state, as seen in Fig. 15. For pure quark stars, the relation is similar but with different parameters, due to the different density-pressure distribution at lower densities. But if only nuclear, hyperon matter, and hybrid stars are considered,

the empirical relation is universal for these families of equations of state. If the mass of the star emitting the gravitational wave is known by other measurements, this relation could be used to obtain the radius of the star emitting the gravitational wave. Following a procedure similar to the one explained previously for the wI modes, a detection of frequency and damping time of a neutron star emission, for which the mass is already known by other measurements, would draw a horizontal line in Fig. 15. The intersection of this line with the empirical relation (30) would provide an estimation of the radius of the star.

Suppose that for the previous measurement of the wI0 mode we also have a measurement of the f mode, with  $\omega = 1.9$  kHz and  $\tau = 0.3$  s. If the corresponding mass of the star is  $M = 1.479 M_\odot$ , we can trace the horizontal line of Fig. 15. The intersection of this line with empirical relation (30) determines the radius of the star,  $R = 11.53$  km.

The previous values of wI0 modes, f modes, and mass we have used for these estimation examples correspond to a real configuration of the SLy equation of state. This configuration has central pressure  $p_c = 1.58 \times 10^{35}$  dyn/cm<sup>2</sup> and radius  $R = 11.6$  km. Note that the error in the determination of the central pressure has been 17%, but, nevertheless, in the determination of the radius of the star, the error is 0.5%.

Combining the two empirical relations (29) and (30), the particular equation of state of the source of the detected emission could be constrained.

## V. CONCLUSIONS

In this paper, we have considered the polar quasinormal modes for realistic neutron stars. In particular, we have calculated the fundamental wI mode, the f mode, and the fundamental p mode. The study has been realized for 15 realistic equations of state, all of them satisfying the  $2 M_\odot$  condition, and various compositions: hyperon, hybrid, and pure quark matter. We have calculated the quasinormal modes also for the SLy equation of state in order to compare it to a standard nucleonic equation of state. The numerical procedure developed to obtain the quasinormal modes is based on exterior complex scaling. A similar study for the axial part of the spectrum can be found in Ref. [35].

We have considered empirical relations between the scaled frequencies and damping times of the modes with the compactness and mean density. The results are in accordance with previous works [16]. We have studied in which cases the obtained relations are more independent of the equation of state and, hence, more useful for asteroseismology. We have found that the frequencies of the fundamental p mode and f mode are quite sensitive to the matter composition of the star, so these empirical relations are less useful.

New phenomenological relations have been studied, for the fundamental wI mode and f mode, between the real part



and the imaginary part of the fundamental modes. We have found universal empirical relations, independent of the particular equation of state. These relations can be useful in neutron star asteroseismology, allowing us to constrain the equation of state and so providing insight into the state of matter at high densities.

### ACKNOWLEDGMENTS

We would like to thank I. Bednarek for kindly providing us with the equation of state BHZBM, I. Sagert for

equations of state WSPHS1–WSPHS3, A. Sedrakian for equations of state BS1–BS4, and S. Weissenborn for equations of state WCS1–WCS2. We thank Daniela Doneva for valuable comments on our work and Gabriel A. Galindo for his help concerning the exterior complex scaling method. We would also like to thank the referee for his/her suggestions. This work was supported by the Spanish Ministerio de Ciencia e Innovacion, research Project No. FIS2011-28013. J.L.B. was supported by the Spanish Universidad Complutense de Madrid.

- 
- [1] A. Haensel, P. Potekhin, and D. Yakovlev, *Neutron Stars: Equation of State and Structure*, Astrophysics and Space Science Library (Springer, New York, 2007).
- [2] N. Glendenning, *Compact Stars: Nuclear Physics, Particle Physics, and General Relativity*, Astronomy and Astrophysics Library (Springer, New York, 2000).
- [3] H. Heiselberg and M. Hjorth-Jensen, *Phys. Rep.* **328**, 237 (2000).
- [4] M. Prakash and J.M. Lattimer, *From Nuclei to Stars*, edited by S. Lee (World Scientific, Singapore, 2011), Chap. 12, p. 275–304.
- [5] I. Bednarek, P. Haensel, J.L. Zdunik, M. Bejger, and R. Mañka, *Astron. Astrophys.* **543**, A157 (2012).
- [6] L. Bonanno and A. Sedrakian, *Astron. Astrophys.* **539**, A16 (2012).
- [7] S. Weissenborn, D. Chatterjee, and J. Schaffner-Bielich, *Phys. Rev. C* **85**, 065802 (2012).
- [8] S. Weissenborn, I. Sagert, G. Pagliara, M. Hempel, and J. Schaffner-Bielich, *Astrophys. J. Lett.* **740**, L14 (2011).
- [9] B. Sathyaprakash and B. F. Schutz, *Living Rev. Relativity* **12**, 1 (2009).
- [10] M. Pitkin, S. Reid, S. Rowan, and J. Hough, *Living Rev. Relativity* **14**, 1 (2011).
- [11] K.D. Kokkotas and B. Schmidt, *Living Rev. Relativity* **2**, 1 (1999).
- [12] H.-P. Nollert, *Classical Quantum Gravity* **16**, R159 (1999).
- [13] L. Rezzolla, *Gravitational Waves from Perturbed Black Holes and Relativistic Stars* (ICTP, Trieste, 2003).
- [14] O. Benhar, E. Berti, and V. Ferrari, *Mon. Not. R. Astron. Soc.* **310**, 797 (1999).
- [15] K.D. Kokkotas, T.A. Apostolatos, and N. Andersson, *Mon. Not. R. Astron. Soc.* **320**, 307 (2001).
- [16] O. Benhar, V. Ferrari, and L. Gualtieri, *Phys. Rev. D* **70**, 124015 (2004).
- [17] O. Benhar, *Mod. Phys. Lett. A* **20**, 2335 (2005).
- [18] V. Ferrari and L. Gualtieri, *Gen. Relativ. Gravit.* **40**, 945 (2008).
- [19] D. Chatterjee and D. Bandyopadhyay, *Phys. Rev. D* **80**, 023011 (2009).
- [20] D.-H. Wen, B.-A. Li, and P.G. Krastev, *Phys. Rev. C* **80**, 025801 (2009).
- [21] T. Regge and J. A. Wheeler, *Phys. Rev.* **108**, 1063 (1957).
- [22] F.J. Zerilli, *Phys. Rev. Lett.* **24**, 737 (1970).
- [23] K. Thorne and A. Campolattaro, *Astrophys. J.* **149**, 591 (1967).
- [24] R. Price and K. Thorne, *Astrophys. J.* **155**, 163 (1969).
- [25] K. Thorne, *Astrophys. J.* **158**, 1 (1969).
- [26] K. Thorne, *Astrophys. J.* **158**, 997 (1969).
- [27] A. Campolattaro and K. Thorne, *Astrophys. J.* **159**, 847 (1970).
- [28] L. Lindblom and S. Detweiler, *Astrophys. J. Suppl. Ser.* **53**, 73 (1983).
- [29] S. Detweiler and L. Lindblom, *Astrophys. J.* **292**, 12 (1985).
- [30] S. Chandrasekhar and V. Ferrari, *Proc. R. Soc. A* **432**, 247 (1991).
- [31] S. Chandrasekhar, V. Ferrari, and R. Winston, *Proc. R. Soc. A* **434**, 635 (1991).
- [32] S. Chandrasekhar and V. Ferrari, *Proc. R. Soc. A* **434**, 449 (1991).
- [33] J.R. Ipser and R.H. Price, *Phys. Rev. D* **43**, 1768 (1991).
- [34] Y. Kojima, *Phys. Rev. D* **46**, 4289 (1992).
- [35] J.L. Blázquez-Salcedo, L.M. González-Romero, and F. Navarro-Lérida, *Phys. Rev. D* **87**, 104042 (2013).
- [36] K.D. Kokkotas and B.F. Schutz, *Mon. Not. R. Astron. Soc.* **255**, 119 (1992).
- [37] N. Andersson, K.D. Kokkotas, and B.F. Schutz, *Mon. Not. R. Astron. Soc.* **274**, 9 (1995).
- [38] K.D. Kokkotas, *Mon. Not. R. Astron. Soc.* **268**, 1015 (1994).
- [39] L. Samuelsson, N. Andersson, and A. Maniopoulou, *Classical Quantum Gravity* **24**, 4147 (2007).
- [40] N. Andersson and K.D. Kokkotas, *Phys. Rev. Lett.* **77**, 4134 (1996).
- [41] N. Andersson and K.D. Kokkotas, *Mon. Not. R. Astron. Soc.* **299**, 1059 (1998).
- [42] O. Benhar, V. Ferrari, L. Gualtieri, and S. Marassi, *Gen. Relativ. Gravit.* **39**, 1323 (2007).
- [43] N. Andersson, *Proc. R. Soc. A* **439**, 47 (1992).
- [44] J. Aguilar and J. Combes, *Commun. Math. Phys.* **22**, 269 (1971).
- [45] E. Balslev and J. Combes, *Commun. Math. Phys.* **22**, 280 (1971).
- [46] B. Simon, *Commun. Math. Phys.* **27**, 1 (1972).
- [47] J.S. Read, B.D. Lackey, B.J. Owen, and J.L. Friedman, *Phys. Rev. D* **79**, 124032 (2009).

- [48] F. Douchin and P. Haensel, *Astron. Astrophys.* **380**, 151 (2001).
- [49] F. Fritsch and R. Carlson, *SIAM J. Numer. Anal.* **17**, 238 (1980).
- [50] U. Ascher, J. Christiansen, and R.D. Russell, *Math. Comput.* **33**, 659 (1979).
- [51] C. Misner, K. Thorne, and J. Wheeler, *Gravitation*, Physics Series (Freeman, San Francisco, 1973).
- [52] Y. Kojima, N. Andersson, and K.D. Kokkotas, *Proc. R. Soc. A* **451**, 341 (1995).
- [53] N. Glendenning, *Astrophys. J.* **293**, 470 (1985).
- [54] B.D. Lackey, M. Nayyar, and B.J. Owen, *Phys. Rev. D* **73**, 024021 (2006).
- [55] M. Alford, M. Braby, M. Paris, and S. Reddy, *Astrophys. J.* **629**, 969 (2005).